ZFP36 ring finger protein like 1 significantly suppresses human coronavirus OC43 replication

Tooba Momin [1], Andrew Villasenor [1], Amit Singh [1], Mahmoud Darweesh [2], Aditi Singh [1], Mrigendra Rajput [Corresp. 1]

[1] Department of Biology, University of Dayton, Dayton, Ohio, United States

[2] Department of Medical Biochemistry and Microbiology, Uppsala University, Uppsala, Uppsala, Sweden

Corresponding Author: Mrigendra Rajput
Email address: mrajput1@udayton.edu

CCCH-type Zinc figure proteins (ZFP) are small cellular proteins that are structurally maintained by zinc ions. Zinc ions coordinate the protein structure in a tetrahedral geometry by binding to cystine- cystine or cysteines - histidine amino acids. ZFP's unique structure enables it to interact with a wide variety of molecules including RNA; thus, ZFP modulates several cellular processes including the host immune response and virus replication. CCCH-type ZFPs have shown their antiviral efficacy against several DNA and RNA viruses. However, their role in the human coronavirus is little explored. We hypothesized that ZFP36L1 also suppresses the human coronavirus. To test our hypothesis, we used OC43 human coronavirus (HCoV) strain in our study. We overexpressed and knockdown ZFP36L1 in HCT-8 cells using lentivirus transduction. Wild type, ZFP36L1 overexpressed, and ZFP36L1 knockdown cells were each infected with HCoV-OC43, and the virus titer in each cell line was measured over 96 hours post-infection (p.i.). Our results show that HCoV-OC43 replication was significantly reduced with ZFP36L1 overexpression while ZFP36L1 knockdown significantly enhanced virus replication. ZFP36L1 knockdown HCT-8 cells started producing infectious virus at 48 hours p.i. which was an earlier timepoint as compared to wild -type and ZFP36L1 overexpressed cells. Wild-type and ZFP36L1 overexpressed HCT-8 cells started producing infectious virus at 72 hours p.i.. Overall, the current study showed that overexpression of ZFP36L1 suppressed human coronavirus (OC43) production.

1 ZFP36 Ring Finger Protein Like 1 significantly suppresses
2 Human coronavirus OC43 replication

4 Tooba Momin[1], Andrew Villasenor[1], Amit Singh[1], Mahmoud Darweesh[2], Aditi Singh[1],
5 Mrigendra Rajput[1]
6
7
8 [1] Department of Biology, University of Dayton, Dayton, Ohio, USA 45469

9 [2] Department of Medical Biochemistry and Microbiology, Uppsala University, Uppsala, Sweden,

10 75105

12
13 Corresponding Author:
14 Mrigendra Rajput
15 SC 234, Department of Biology, 300 College Street, University of Dayton, Dayton, Ohio, 45469,
16 USA

18
19
20
21
22
23
24
25
26
27
28
29
30
31
32
33
34
35
36
37

Abstract

38

39   CCCH-type Zinc figure proteins (ZFP) are small cellular proteins that are structurally maintained

40   by zinc ions. Zinc ions coordinate the protein structure in a tetrahedral geometry by binding to

41   cystine- cystine or cysteines - histidine amino acids. ZFP's unique structure enables it to interact

42   with a wide variety of molecules including RNA; thus, ZFP modulates several cellular processes

43   including the host immune response and virus replication. CCCH-type ZFPs have shown their

44   antiviral efficacy against several DNA and RNA viruses. However, their role in the human

45   coronavirus is little explored. We hypothesized that ZFP36L1 also suppresses the human

46   coronavirus. To test our hypothesis, we used OC43 human coronavirus (HCoV) strain in our

47   study. We overexpressed and knockdown ZFP36L1 in HCT-8 cells using lentivirus transduction.

48   Wild type, ZFP36L1 overexpressed, and ZFP36L1 knockdown cells were each infected with

49   HCoV-OC43, and the virus titer in each cell line was measured over 96 hours post-infection

50   (p.i.).

51   Our results show that HCoV-OC43 replication was significantly reduced with ZFP36L1

52   overexpression while ZFP36L1 knockdown significantly enhanced virus replication. ZFP36L1

53   knockdown HCT-8 cells started producing infectious virus at 48 hours p.i. which was an earlier

54   timepoint as compared to wild -type and ZFP36L1 overexpressed cells. Wild-type and ZFP36L1

55   overexpressed HCT-8 cells started producing infectious virus at 72 hours p.i.. Overall, the

56   current study showed that overexpression of ZFP36L1 suppressed human coronavirus (OC43)

57   production.

58
59
60
61

62   Keywords: CCCH type Zinc finger protein, ZFP36L1, RNA binding protein, human coronavirus

63   OC43

Introduction

ZFPs are small cellular proteins that are structurally maintained by zinc ions. Zinc ions coordinate the protein structure in a tetrahedral geometry (Abbehausen, 2019; Hajikhezri, 2020). There are over 40 different types of ZFPs that have been annotated so far (Hajikhezri, 2020). ZFP's unique structure enables it to interact with a wide variety of molecules such as DNA, RNA, PAR (poly-ADP-ribose), and cellular proteins and thus modulate several cellular processes including host immune response and virus replication (Müller et al., 2007; Cassandri et al., 2017; Takata et al., 2017; Tang, Wang & Gao, 2017; Meagher et al., 2019;Lal, Ullah & Syed, 2020; Nchioua et al., 2020; Gonzalez-Perez et al., 2021; Wang & Zheng, 2021). Among various ZFPs, the CCCH-type ZFP family contains zinc ions that coordinate protein structure by binding to cystine-cystine or cysteines-histidine amino acids (Abbehausen, 2019; Hajikhezri, 2020). The CCCH-type ZFP family has also been characterized for its antiviral (Hajikhezri, 2020; Tang, Wang & Gao, 2017; Zhang, et al., 2020; Guo et al ., 2004; Zhao et al., 2019; Gao, Guo & Goff, 2002; Zhu et al., 2020; Musah, 2004; Chen, Jeng & Lai, 2017; Scozzafava et al., 2003; Schito et al., 2006; Angiolilli et al., 2021) and immune modulator activity (Wang et al., 2015; Tu et al., 2019; Haneklaus et al., 2017; Lv et al., 2021; Matsushita et al., 2009; Wawro, Kochan & Kasza, 2016; Uehata, & Akira, 2013; Chen et al., 2018; Mino et al., 2015; Fu & Blackshear, 2017; Stumpo, Lai & Blackshear, 2010; Shrestha, Pun & Park, 2018; Kontoyiannis, 2018; Chiu et al., 2022).

CCCH-type ZFPs show their antiviral efficacy against several RNA viruses including Influenza A virus (Tang, Wang & Gao, 2017), retrovirus (Gao, Guo & Goff, 2002; Zhu et al., 2011; Zhu et al., 2017) filoviruses (Müller, 2007), and alphavirus such as Sindbis virus, Semliki Forest virus, Ross River virus, and Venezuelan equine encephalitis virus (Bick et al., 2003). However, CCCH-type ZFP's role on the human coronavirus is little explored. The current study is designed to evaluate the effect of ZFP36L1, a CCCH-type ZFP, on human coronavirus (HCoV)-OC43 replication.

88 **Materials & Methods**

89

90 **Cells, Virus Strains and Virus Propagation**

91 HCT-8 cells (ATCC, Manassas, VA) were cultured in Roswell Park Memorial Institute (RPMI)

92 1640 Medium (Gibco BRL, Grand Island, NY) and supplemented with 10% heat-inactivated

93 fetal bovine serum (FBS), (ATCC, Manassas, VA), and antibiotic-antimycotic: penicillin 100

94 units /ml, streptomycin 0.10 mg /ml and amphotericin B 0.25 μg /ml (Sigma-Aldrich, St. Louis,

95 MO). During virus culture, HCT-8 cells were adapted to 1% FBS. HCT-8 cells cultured with

96 RPMI 1640 medium supplemented with 1% FBS were used to grow and subsequently titrate the

97 OC43 human coronavirus (HCoV) stain (ATCC, Manassas, VA).

98 **Overexpression and knockdown of ZFP36L1**

99 HCT-8 cells were stably overexpressed for ZFP36L1 (NCBI reference sequence:

100 NM_001244701.1) with a green fluorescent protein (GFP) marker using a lentivirus vector. The

101 ZFP36L1 gene containing both tandem zinc finger domains (TZFD) such as TZFD1 and TZFD2

102 were cloned in a pLV-eGFP plasmid with the help of Vector Builder Inc, IL. To make the

103 lentivirus, pLV-eGFP plasmids containing our gene of interest were co-transfected with VSV-G

104 and packaging plasmids encoding Gag/Pol and Rev in HEK293T cells. After 48 hours, the

105 supernatant containing the lentivirus was collected and purified by centrifugation followed by

106 filtration. Purified lentivirus was concentrated using a sucrose gradient ultracentrifugation and

107 this concentrated, purified lentivirus was used in the study.

108 Similar to ZFP36L1 overexpression, HCT-8 cells were knockdown for ZFP36L1 using ZFP36L1

109 specific shRNA (GTAACAAGATGCTCAACTATA). The ZFP36L1 shRNA was stably

110 expressed using a lentivirus by cloning it in a pLV-mCherry plasmid. Lentivirus for ZFP36L1-

111   shRNA was prepared as per the above-mentioned method by co-transfection of pLV-mCherry

112   containing ZFP36L1 shRNA with VSV-G and packaging plasmids in HEK293T cells.

113   The prepared lentiviruses were used to either overexpress or knock down ZFP36L1. Successful

114   lentivirus transduction was measured through GFP or mCherry expression for ZFP36L1

115   overexpression (GFP) or ZFP36L1knockdown (mCherry), respectively. Transduced HCT-8 cells

116   were selected with an increased concentration of puromycin (2-3 μg/ml) over 7 days. Selected

117   cells were further characterized for ZFP36L1 overexpression or knockdown using a western blot

118   with ZFP36L1-specific antibodies.

119   **Western blot analysis for ZFP36L1 expression**

120   To confirm ZFP36L1 overexpression or ZFP36L1 knockdown; wild type, ZFP36L1

121   overexpressed and ZFP36L1 knockdown HCT-8 cells were individually seeded in T25 flasks.

122   When cells reached 75-80% confluency, cells were lysed using a radioimmunoprecipitation

123   assay buffer (RIPA buffer) (Cell Signaling Technology, Danvers, MA) supplemented with

124   protease-phosphatase inhibitor (Cell Signaling Technology, Danvers, MA). Lysates were then

125   centrifuged at 3000 X g for 15 minutes at 4 °C. The supernatant was collected and the protein

126   concentration in each supernatant was measured using the Pierce™ BCA Protein Assay Kit

127   (Thermo Fisher Scientific, Waltham, MA). 40 μg cell lysates were separated through 12%

128   resolving SDS PAGE gel. After separation, proteins were transfected onto a polyvinylidene

129   difluoride (PVDF) membrane (Thermo Fisher Scientific, Waltham, MA). The PVDF membrane

130   was blocked with 5% skimmed milk (Sigma-Aldrich, St. Louis, MO) in Tris-buffered saline

131   (TBS) for 1 hour at room temperature followed by incubation with anti- ZFP36L1 antibody

132   (1:1000) (Thermo Fisher Scientific, Waltham, MA) and anti- βactin antibody (1:4000) (Cell

133   Signaling Technology, Danvers, MA) overnight at 4 °C. After overnight incubation, membranes

134   were washed with tris-buffered saline +0.1% Tween 20 (TBST) and incubated with HRP

135   conjugated secondary antibodies (1:2000) for 1 hour at room temperature. After washing,

136   membranes were developed using the Pierce ECL Western Blotting Substrate (Thermo Fisher

137   Scientific, Waltham, MA). Images of the western blot were taken by the Odyssey XF Imaging

138   System (LI-COR Biosciences, Lincoln, NE). Band intensity for ZFP36L1 proteins was

139   normalized with β actin using ImageJ software (Schneider, Rasband & Eliceiri, 2012) A

140   significant difference in ZFP36L1 expression in ZFP36L1 overexpressed and knockdown cells

141   compared to wild-type cells was estimated using a paired T-test.

142   **Determining ZFP36L1's effect on HCT-8 cells viability**

143   The effect of ZFP36L1 overexpression and its knockdown on cell viability was measured by

144   trypan blue exclusion assay (Strober, 2015). Wild type, ZFP36L1 overexpressed and ZFP36L1

145   knockdown cells were individually seeded in 6 well plates (1.5×10^6 cell/well) in triplicate. 96

146   hours post-seeding, cells were washed with sterilized phosphate-buffered saline (PBS) and

147   detached with 0.25% trypsin-EDTA (ATCC, Manassas, VA). Detached cells were washed with

148   PBS by centrifugation at 500x g for 5 minutes at 4 °C, and then cells were stained with 0.4%

149   trypan blue for 3 minutes and examined for cell. Changes in cell viability following ZFP36L1

150   overexpression or its knockdown compared to wild-type cells was estimated by paired t-test.

151   **Measuring the effect of ZFP36L1 expression on virus titration**

152   Wild type, ZFP36L1 overexpressed and ZFP36L1 knockdown HCT-8 cells were infected with

153   HCoV-OC43 with 0.1 multiple of infection (MOI) individually. The supernatant from these cells

154   was collected at 24 hours, 48 hours, 72 hours, and 96 hours p.i. Collected cell supernatants were

155   then centrifuged at 1000Xg at 4°C for 15 minutes to remove cell debris and stored at -80 ° C

156   until used. Once samples from all time points were collected, the HCoV-OC43 virus titer was

157   determined as per the aforementioned method (Reed & Muench, 1938). Changes in virus titer in

158   ZFP36L1 overexpressed or ZFP36L1 knockdown cells were compared to wild-type cells and

159   statistically analyzed by a paired T-test.

160   **Measuring the effect of ZFP36L1 expression on HCoV-OC43 replication.**

161   To measure the effect of ZFP36L1 overexpression or ZFP36L1 knockdown on HCoV-OC43

162   replication, we infected ZFP36L1 overexpressed, ZFP36L1 knockdown or wild type HCT-8 cells

163   with HCoV-OC43 (MOI: 0.1). Infected cells were collected at 72 and 96 hours p.i. Viral RNA

164   was isolated from infected cells using the QIAamp Viral RNA Mini kit (Qiagen, Valencia, CA,

165   USA). The viral nucleocapsid was quantified using qPCR (Stratagene MX3000P Real-Time

166   Thermocycler, Stratagene Inc., La Jolla, USA) in 25 μl reaction using syber green dye. Primer

167   sequence for nucleocapsid (F: 5'-: GCTGTT TWTGTTAAG TCYAAA GT-3', R: 5'-

168   ATTCTGATAGAGAGTGCYTAT Y-3') were used (Al-Khannaq, et al., 2016) with qPCR

169   amplification cycle at 95°C/ 2 minutes, 40 cycles of (95 °C/15 and 60 °C/ 1 minutes) followed

170   by melting curve cycle at: 95°C/ 15 seconds, 60°C/ 1 minute and 95°C/ 15 seconds. Fold change

171   in HCoV nucleocapsid expression in each cell was estimated by paired -test.

172   **Statistical analysis**

173   The significant change in HCoV-OC43 titer and virus replication in wild-type, ZFP36L1

174   overexpressed, or ZFP36L1 knockdown cells was estimated using a paired T-test with 95%

175   degree of freedom. Virus titer in wild-type, ZFP36L1 overexpression or ZFP36L1 knockdown

176   cells was repeated at least three times with calculations for average, standard deviation, and

177   standard error.

178
179   **Results**
180
181   **ZFP36L1 was overexpressed or knockdown in HCT-8 cells.**

182   A stable ZFP36L1 overexpression with an upstream GFP marker in HCT-8 cells was generated

183   using a lentivirus system. GFP expression in HCT-8 cells was considered positive for ZFP36L1

184   overexpression (Figure 1B), which was further confirmed by western blot (Figure 2 and Figure

185   3). Similarly, ZFP36L1 was knockdown using ZFP36L1-specific shRNA. The shRNA was

186   located downstream to mCherry and expression of ZFP36L1-specific shRNA was determined by

187   mCherry expression (Figure 1C) and ZFP36L1 knockdown was confirmed by western blot

188   analysis (Figure 2 and Figure 3). Our results showed that lentivirus significantly overexpressed

189   or knockdown ZFP36L1 in HCT-8 cells ($p < 0.05$) (Figure 2 and Figure 3).

190

191   **ZFP36L1 overexpressing or its knockdown did not affect HCT-8 cells' viability**

192   The effect of ZFP36L1 overexpression or its knockdown was measured on HCT-8 cells' viability

193   using trypan blue exclusion assay. Results showed that overexpression or knockdown of

194   ZFP36L1 in HCT-8 cells did not affect its viability. Wild type, ZFP36L1 overexpressed and

195   ZFP36L1 knockdown cells showed viability as 94.83±1.01%, 94.16±0.71%, and 95.83±0.43% at

196   96 hours post seeding, respectively These values were non-significant different to each other

197   ($p < 0.05$) (Figure 4). Additionally, no apparent morphological changes were observed among

198   these cells.

199   **ZFP36L1 overexpression significantly suppressed while ZFP36L1 knockdown significantly**

200   **enhanced the HCoV-OC43 production.**

201   Wild type,ZFP36L1 overexpressed, and ZFP36L1 knockdown HCT-8 cells were infected

202   individually with HCoV-OC43 with MOI of 0.1. Cell supernatants were collected at 24 hours, 48

203   hours, 72 hours, and 96 hours p.i. and analyzed for virus titer.

204 Results showed that ZFP36L1 overexpression in HCT-8 cells significantly reduced virus titer

205 (p<0.05) (Figure 5). Virus titer in ZFP36L1 overexpressed cells ion was 2.24±1.28 log10/ml and

206 4.32±0.00 log10/ml at 72 hours and 96 hours p.i. respectively. These titer values were

207 significantly lower than virus titers in wild-type cells at same time points, such as 72 hours p.i.

208 (4.08±0.11 log 10/ml) and 96 hours p.i. (5.42±0.10 log 10/ml) (p<0.05) (Figure 5).

209 Results with ZFP36L1 knockdown HCT-8 cells showed that ZFP36L1 knockdown significantly

210 enhanced virus titer (p<0.05) (Figure 5). Knocking down ZFP36L1 facilitated the infectious

211 virus production as early as 48 hours p.i. while wild-type cells produced infectious viruses at 72

212 hours p.i. The virus titer in ZFP36L1 knockdown cells was recorded as 00.00±0.00 log 10/ml,

213 2.86±0.00 log 10/ml, 4.52±0.22 log 10/ml, and 5.85±0.01 log 10/ml at 24 hours, 48 hours, 72

214 hours and 96 hours p.i., respectively. While wild-type HCT-8 cells have virus titer of 0.00±0.00

215 log 10/ml, 0.00±0.00 log 10/ml, 4.08±0.11 log 10/ml, and 5.42±0.10 log 10/ml at 24 hours, 48

216 hours, 72 hours and 96 hours p.i., respectively. Virus titer in ZFP36L1 knockdown cells was

217 significantly higher at 48 hours and 96 hours p.i compared to wild-type cells (p<0.05) (Figure 5).

218 Results also showed a lower cytopathic effect in ZFP36L1 overexpressed or wild-type HCT-8

219 cells compared to ZFP36L1 knockdown cells at 72 hours p.i. (Figure 6)

220 **ZFP36L1 overexpression significantly suppressed while ZFP36L1 knockdown significantly**

221 **enhanced the HCoV-OC43 RNA replication.**

222 To further confirm ZFP36L1's effect on HCoV-OC43 RNA replication, wild type, ZFP36L1

223 overexpressed and ZFP36L1 knockdown HCT-8 cells were individually infected with HCoV-

224 OC43 (MOI: 0.1). Infected cells were collected at 72 and 96 hours p.i. Viral RNA was isolated

225 from infected cells and viral nucleocapsid transcription (RNA concentration) was analyzed using

226 qPCR. Results did not show any significant difference in HCoV-OC43 nucleocapsid RNA

227 concentration among these cells at 72 hours p.i. However, at 96 hours p.i. ZFP36L1 knockdown

228 HCT-8 cells showed significantly higher HCoV-OC43 nucleocapsid transcription compared to

229 wild type HCT-8 cells (p<0.05). ZFP36L1 knockdown HCT-8 cells displayed an 11.14±2.21-

230 fold increase in HCoV-OC43 nucleocapsid RNA compared to wild-type HCT-8 cells. While

231 ZFP36L1 overexpressed cells displayed a significantly lower HCoV-OC43 nucleocapsid RNA

232 (0.37±0.13 fold) compared to wild-type cells at 96 hours p.i. (p<0.05) (Figure 7).

233 **Discussion**
234 The current study was designed to determine the role of ZFP36L1 (a CCCH type ZFP) on

235 HCoV-OC43 replication. Our results showed that overexpression of ZFP36L1 significantly

236 reduced infectious HCoV-OC43 production while ZFP36L1 knockdown significantly enhanced

237 virus titer compared to wild-type cells. ZFP36L1 overexpression also reduced the RNA

238 replication of HCoV-OC43 and suppressed the apparent cytopathic effect in infected cells.

239 ZFPs are one of the most abundant proteins in humans which can make up to 5% of total human

240 proteins (Vilas et al., 2018). ZFPs have an extremely high binding ability. They can bind to cellular

241 DNA, RNA, lipids, proteins, and PAR (poly-ADP-ribose); therefore, ZFPs can modulate several

242 cellular types of machinery (Müller et al., 2007; Cassandri et al., 2017; Takata et al., 2017; Tang,

243 Wang & Gao, 2017; Vilas et al., 2018; Meagher et al., 2019; Lal, Ullah & Syed, 2020; Nchioua et

244 al., 2020, Wang & Zheng, 2021; Gonzalez-Perez et al., 2021). The diverse binding properties of

245 ZFPs make it difficult to characterize their functional effect in cells (Vilas et al., 2018). However,

246 such a challenge is overcome by classifying the ZFPs and then identifying their functional

247 characteristics (Cassandri et al., 2017). Classification of ZFP is based on zinc ion, zinc ion

248 interaction with specific amino acids, and the protein's folded structure (Krishna, Majumdar &

249 Grishin, 2003). Based on such classification, CCCH-type ZFP is characterized to interact with

250   RNA and thus modulate RNA metabolism in the cell (Maeda & Akira, 2017). including interfering

251   with RNA virus replication (Gao, Guo & Goff, 2002; Cassandri et al., 2017).

252   The known mechanisms by which CCCH-type ZFPs exhibit these antiviral or immunomodulatory

253   activities is by limiting the total mRNA turnover in the cell. CCCH-type ZFPs such as ZFP36L1

254   have two tandem zinc finger (TZF) domains that are known to bind with adenyl and uracyl

255   nucleotides-rich (AU-rich) elements (AREs) in mRNA. This interaction facilitates RNA

256   degradation by CCR4-NOT complex-mediated deadenylation, followed by 5' decapping and

257   exonuclease-mediated nucleotide cleaving (Blackshear, 2002; Lai, Kennington & Blackshear,

258   2003; Lykke-Andersen & Wagner, 2005; Suk et al., 2018; Lai et al., 2019; Lai et al., 2000; Chiu

259   et al., 2022).

260   Coronavirus genome, including HCoV-OC43's genome is 5'-capped with a 3' poly(A) tail of

261   variable length (Fehr & Perlman, 2015). The length of the poly (A) tail varies at different stages

262   of the virus replication cycle and viruses with longer poly (A) tails replicate at a faster rate (Wu et

263   al., 2013). Therefore, the effect of ZFP36L1 on viral poly (A) may explain reduced virus

264   production with ZFP36L1 overexpression in the current study. Our study not only showed that

265   ZFP36L1 suppressed the infectious HCoV-OC43 production, but also reduced HCoV-OC43

266   nucleocapsid transcription indicating that ZFP36L1 mediates its antiviral effect by limiting the

267   viral RNA in infected cells.

268   However, there is the possibility that ZFP36L1 can reduce virus replication with different

269   mechanisms other than poly A tail interaction. A study showed that CCCH Type ZFP also targets

270   the non-ARE sequence of 3' and 5' (untranslated region) UTR in mRNA (Li et al., 2015). While

271   another study showed that CCCH Type ZFP targets CG-rich viral sequences (Meagher et al.,

272   2019). The study also showed that ZFP36 (ZFP36L1) suppressed the virus production (influenza

273 A virus) by interfering with viral protein translation/ export from the nucleus to the cytoplasm

274 without affecting viral RNA replication (Lin et al., 2020). Therefore, a detailed study to determine

275 ZFP36L1's mechanism of action for suppressing coronavirus replication needs to be explored.

276

277 Conclusions

278 The current study showed that overexpression of ZFP36L1, a CCCH type ZFP significantly

279 reduced HCoV-OC43 RNA (nucleocapsid) and infectious virus production. A reduced viral

280 production was in correlation with reduced cytopathic effect in the infected cells. Furthermore,

281 ZFP36L1 knockdown significantly enhanced the HCoV-OC43 replication and infectious virus

282 production. However, additional mechanisms employed to reduce virus replication still need to

283 be explored.

284

285 Acknowledgments

286 The author thanks the Department of Biology, University of Dayton, Ohio, USA, for providing

287 support to conduct the current research.

288

References

290

291 1. Abbehausen C. 2019. Zinc finger domains as therapeutic targets for metal-based
292   compounds - an update. *Metallomics* 11(1): 15-28.
293 2. Al-Khannaq MN, Ng KT, Oong XY, Pang YK, Takebe Y, Chook JB, Hanafi NS,
294   Kamarulzaman A, Tee KK.2016. Molecular epidemiology and evolutionary histories
295   of human coronavirus OC43 and HKU1 among patients with upper respiratory tract
296   infections in Kuala Lumpur, Malaysia. *Virology Journal*. 25;13:33. doi:
297   10.1186/s12985-016-0488-4. PMID: 26916286; PMCID: PMC4766700.
298 3. Angiolilli C, Leijten EFA, Bekker CPJ, Eeftink E, Giovannone B, Nordkamp MO, van
299   der Wal M, Thijs JL, Vastert SJ, van Wijk F, Radstake TRDJ and van Loosdregt J.
300   2021. ZFP36 family members regulate the pro-inflammatory features of psoriatic
301   dermal fibroblasts. *Journal of Investigative Dermatology*. 142(2):402-413
302 4. Bick MJ, Carroll JW, Gao G, Goff SP, Rice CM, MacDonald MR. 2003. Expression
303   of the zinc-finger antiviral protein inhibits alphavirus replication. *Journal of
304   Virology*.77(21):11555-62.   doi: 10.1128/jvi.77.21.11555-11562.2003.   PMID:
305   14557641; PMCID: PMC229374.

306   *5.*   Blackshear, PJ. 2002. Tristetraprolin and other CCCH tandem zinc-finger proteins in
307   the regulation of mRNA turnover. *Biochemical Society Transactions.* 30*(6): 945-52.*
308   6.   Cassandri M, Smirnov A, Novelli F, Pitolli C, Agostini M, Malewicz M, Melino G,
309   Raschellà G. 2017. Zinc-finger proteins in health and disease. *Cell Death Discovery.*
310   13;3:17071. doi: 10.1038/cddiscovery.2017.71. PMID: 29152378; PMCID:
311   PMC5683310.
312   7.   Cassandri MA, Smirnov F, Novelli C, Pitoll M, Agostini M, Malewicz GG., Raschellà
313   2017. Zinc-finger proteins in health and disease. *Cell Death Discovery.* 3(1): 17071.
314   8.   Chen SC., Jeng KS, and Lai MMC. 2017. Zinc Finger-Containing Cellular
315   Transcription Corepressor ZBTB25 Promotes Influenza Virus RNA Transcription and
316   Is a Target for Zinc Ejector Drugs. *Journal of Virology.* 91(20).
317   9.   Chen XF, Wu J, Zhang YD, Zhang CX, Chen XT, Sun JH, Chen TX. 2018. Role of
318   Zc3h12a in enhanced IL-6 production by newborn mononuclear cells in response to
319   lipopolysaccharide.   *Pediatrics   &   Neonatology.*   59(3):288-295.   doi:
320   10.1016/j.pedneo.2017.09.006. Epub 2017 Sep 21. PMID: 29054363.
321   10.   Chiu H, Chiu HP, Yu HP, Lin LH, Chen ZP, Lin YL, Lin RJ. 2022. Zinc Finger Protein
322   ZFP36L1 Inhibits Flavivirus Infection by both 5'-3' XRN1 and 3'-5' RNA-Exosome
323   RNA   Decay   Pathways.   *Journal   of   Virology.*   12;96(1):e0166521.   doi:
324   10.1128/JVI.01665-21. Epub 2021 Oct 13. PMID: 34643435; PMCID: PMC8754223.
325   11.   Fehr AR and Perlman S. 2015.Coronaviruses: an overview of their replication and
326   pathogenesis. *Methods in Molecular Biology*, 1282: 1-23.
327   12.   Fu M and Blackshear PJ. 2017. RNA-binding proteins in immune regulation: a focus
328   on CCCH zinc finger proteins. *Nature Reviews Immunology*, 17(2): 130-143.
329   13.   Gao G., Guo X, and Goff SP. 2002.Inhibition of retroviral RNA production by ZAP,
330   a CCCH-type zinc finger protein. *Science*, 297(5587): p. 1703-6.
331   14.   Gonzalez-Perez, AC., Stempel M, Wyler E, Urban C, Piras A, Hennig T, Ganskih S,
332   Wei Y, Heim A, Landthaler M, Pichlmair A, Dölken L, Munschauer M, Erhard F and
333   Brinkmann MM. 2021. The Zinc Finger Antiviral Protein ZAP Restricts Human
334   Cytomegalovirus and Selectively Binds and Destabilizes Viral UL4/UL5 Transcripts.
335   *mBio.* 12(3).
336   15.   Guo X, Carroll JW, Macdonald MR, Goff SP and Gao G. 2004. The zinc finger
337   antiviral protein directly binds to specific viral mRNAs through the CCCH zinc finger
338   motifs. *Journal of Virology.* 78(23): 12781-12787.
339   16.   Hajikhezri Z, Darweesh M, Akusjärvi G, Punga T. 2020. Role of CCCH-Type Zinc
340   Finger Proteins in Human Adenovirus Infections. *Viruses.* 18;12(11):1322. doi:
341   10.3390/v12111322. PMID: 33217981; PMCID: PMC7698620.
342   17.   Haneklaus M, O'Neil JD, Clark AR, Masters SL, O'Neill LAJ. 2017.The RNA-binding
343   protein Tristetraprolin (TTP) is a critical negative regulator of the NLRP3
344   inflammasome. *Journal of Biological Chemistry.* 28;292(17):6869-6881. doi:
345   10.1074/jbc.M116.772947. Epub 2017 Mar 16. PMID: 28302726; PMCID:
346   PMC5409458.
347   18.   Kontoyiannis DL. 2018.An RNA checkpoint that keeps immunological memory at
348   bay. *Nature Immunology.*19(8): 795-797.
349   19.   Kozaki T, Takahama M, Misawa T, Matsuura Y, Akira S, Saitoh T. 2015. Role of
350   zinc-finger anti-viral protein in host defense against Sindbis virus. *International*

351   *Immunology*. 27(7):357-64. doi: 10.1093/intimm/dxv010. Epub 2015 Mar 10. PMID:
352   25758257; PMCID: PMC4565983.

353   20.   Krishna SS., Majumdar I,, and Grishin NV. 2003. Structural classification of zinc
354   fingers: survey and summary. *Nucleic Acids Research*31(2): 532-50.

355   21.   Lai WS, Carballo E, Thorn JM, Kennington EA, Blackshear PJ. 2000. Interactions of
356   CCCH zinc finger proteins with mRNA. Binding of tristetraprolin-related zinc finger
357   proteins to Au-rich elements and destabilization of mRNA. *Journal of Biological*
358   *Chemistry* 9;275(23):17827-37. doi: 10.1074/jbc.M001696200. PMID: 10751406.

359   22.   Lai WS, Kennington EA and Blackshear PJ. 2003. Tristetraprolin and its family
360   members can promote the cell-free deadenylation of AU-rich element-containing
361   mRNAs by poly(A) ribonuclease. *Molecular and Cellular Biology*, 23(11): p. 3798-
362   812.

363   23.   Lai WS, Stumpo DJ, Wells ML, Gruzdev A, Hicks SN, Nicholson CO, Yang Z, Faccio
364   R, Webster MW, Passmore LA, Blackshear PJ. 2019. Importance of the Conserved
365   Carboxyl-Terminal CNOT1 Binding Domain to Tristetraprolin Activity *In Vivo*.
366   *Molecular and Cellular Biolog*y. 39(13):e00029-19. doi: 10.1128/MCB.00029-19.
367   PMID: 31036567; PMCID: PMC6580703.

368   24.   Lal S, Ullah BA, and Syed S. 2020.The Role of Zinc-Finger Antiviral Proteins in
369   Immunity against Viruses. *Molecular Genetics, Microbiology and Virology,* 35(2):
370   78-84.

371   25.   Li M, Yan K, Wei L, Yang J, Lu C, Xiong F, Zheng C, Xu W. 2015. Zinc finger
372   antiviral protein inhibits coxsackievirus B3 virus replication and protects against viral
373   myocarditis. *Antiviral Research*. 123:50-61. doi: 10.1016/j.antiviral.2015.09.001.
374   Epub 2015 Sep 2. PMID: 26343012.

375   26.   Lin RJ, Huang CH, Liu PC, Lin IC, Huang YL, Chen AY, Chiu HP, Shih SR, Lin LH,
376   Lien SP, Yen LC, Liao CL. 2020. Zinc finger protein ZFP36L1 inhibits influenza A
377   virus through translational repression by targeting HA, M and NS RNA transcripts.
378   *Nucleic Acids Research*. 27;48(13):7371-7384. doi: 10.1093/nar/gkaa458. PMID:
379   32556261; PMCID: PMC7367194.

380   27.   Lv L, Qin T, Huang Q, Jiang H, Chen F, Long F, Ren L, Liu J, Xie Y, Zeng M. 2021.
381   Targeting Tristetraprolin Expression or Functional Activity Regulates Inflammatory
382   Response Induced by MSU Crystals. *Frontiers in Immunology*. 16;12:675534. doi:
383   10.3389/fimmu.2021.675534. PMID: 34335573; PMCID: PMC8322984.

384   28.   Lykke-Andersen J. and Wagner E. Recruitment and activation of mRNA decay
385   enzymes by two ARE-mediated decay activation domains in the proteins TTP and
386   BRF-1. *Genes & Development*, 19(3): p. 351-61.

387   29.   Maeda K. and Akira S. 2017.Regulation of mRNA stability by CCCH-type zinc-finger
388   proteins in immune cells. *International Immunology*, 29(4): 149-155.

389   30.   Matsushita K, Takeuchi O, Standley DM, Kumagai Y, Kawagoe T, Miyake T, Satoh
390   T, Kato H, Tsujimura T, Nakamura H, Akira S. 2009. Zc3h12a is an RNase essential
391   for controlling immune responses by regulating mRNA decay. *Nature*.
392   30;458(7242):1185-90. doi: 10.1038/nature07924. Epub 2009 Mar 25. PMID:
393   19322177.

394   31.   Meagher J., Takata M, Gonçalves-Carneiro D, Keane SC, Rebendenne A, Ong H, Orr
395   VK, MacDonald MR, Stuckey JA, Bieniasz PD and Smith JL. 2019. Structure of
396   the zinc-finger antiviral protein in complex with RNA reveals a mechanism for

397 selective targeting of CG-rich viral sequences. *Proceedings of the National Academy*
398 *of Sciences.* 116(48): 24303-24309.
399 32. Mino T, Murakawa Y, Fukao A, Vandenbon A, Wessels HH, Ori D, Uehata T, Tartey
400   S, Akira S, Suzuki Y, Vinuesa CG, Ohler U, Standley DM, Landthaler M, Fujiwara
401   T, Takeuchi O. 2015. Regnase-1 and Roquin Regulate a Common Element in
402   Inflammatory mRNAs by Spatiotemporally Distinct Mechanisms. *Cell.*
403   21;161(5):1058-1073. doi: 10.1016/j.cell.2015.04.029. PMID: 26000482.
404 33. Müller S, Möller P, Bick MJ, Wurr S, Becker S, Günther S and Kümmerer BM. 2007.
405   Inhibition of filovirus replication by the zinc finger antiviral protein. *Journal of*
406   *virology.* 81(5): 2391-2400.
407 34. Musah RA 2004, The HIV-1 nucleocapsid zinc finger protein as a target of
408   antiretroviral therapy. *Current Topics in Medicinal Chemistry*, 4 (15): 1605-22.
409 35. Nchioua R, Kmiec D, Müller JA, Conzelmann C, Groß R, Swanson CM, Neil SJD,
410   Stenger S, Sauter D, Münch J, Sparrer KML and Kirchhoff F. 2020. SARS-CoV-2 Is
411   Restricted by Zinc Finger Antiviral Protein despite Preadaptation to the Low-CpG
412   Environment in Humans. *mBio.* 11(5).
413 36. Reed LJ and Muench J. 1938. A simple method of estimating fifty percent endpoints..
414   *American Journal of Epidemiology.*27(3): 493-497.
415 37. Schito ML, Soloff AC, Slovitz D, Trichel A, Inman JK, Appella E, Turpin JA and
416   Barratt-Boyes SM. 2006. Preclinical evaluation of a zinc finger inhibitor targeting
417   lentivirus nucleocapsid protein in SIV-infected monkeys. *Current HIV Research.* 4(3):
418   379-386.
419 38. Schneider C., Rasband W. and Eliceiri K. 2012. NIH Image to ImageJ: 25 years of
420   image   analysis.   *Nature   Methods*   9,   671–675   (2012).
421   https://doi.org/10.1038/nmeth.2089.
422 39. Scozzafava A., Owa T, Mastrolorenzo A and Supuran CT . 2003. Anticancer and
423   antiviral sulfonamides. *Current Medicinal Chemistry.* 10(11): 925-953.
424 40. Shrestha A, Pun NT and Park PH. 2018.ZFP36L1 and AUF1 Induction Contribute to
425   the Suppression of Inflammatory Mediators Expression by Globular Adiponectin via
426   Autophagy Induction in Macrophages. *Biomolecules & Therapeutics.*26(5): 446-457.
427 41. Strober W. 2015. Trypan Blue Exclusion Test of Cell Viability. *Current Protocols in*
428   *Immunology.* 2;111:A3.B.1-A3.B.3. doi: 10.1002/0471142735.ima03bs111. PMID:
429   26529666; PMCID: PMC6716531
430 42. Stumpo DJ., Lai WS, and Blackshear PJ. 2010. Inflammation: cytokines and RNA-
431   based regulation. *Wiley Interdisciplinary Reviews:RNA*, 1(1): 60-80.
432 43. Suk FM, Chang CC, Lin RJ, Lin SY, Liu SC, Jau CF, Liang YC. 2018. ZFP36L1 and
433   ZFP36L2 inhibit cell proliferation in a cyclin D-dependent and p53-independent
434   manner. *Scientific Reports.* 9;8(1):2742. doi: 10.1038/s41598-018-21160-z. Erratum
435   in: Sci Rep. 2019 Nov 20;9(1):17457. PMID: 29426877; PMCID: PMC5807420.
436 44. Takata MA, Gonçalves-Carneiro D, Zang TM, Soll SJ, York A, Blanco-Melo D and
437   Bieniasz PD. 2017. CG dinucleotide suppression enables antiviral defence targeting
438   non-self RNA. *Nature.* 550(7674): 124-127.Tu Y, Wu X, Yu F, Dang J, Wang J, Wei
439   Y, Cai Z, Zhou Z, Liao W, Li L, Zhang Y. 2019. Tristetraprolin specifically regulates
440   the expression and alternative splicing of immune response genes in HeLa cells. *BMC*
441   *Immunology.* 2;20(1):13. doi: 10.1186/s12865-019-0292-1. PMID: 31046669;
442   PMCID: PMC6498542.

45. Tang Q, Wang X, and Gao G. 2017. The Short Form of the Zinc Finger Antiviral Protein Inhibits Influenza A Virus Protein Expression and Is Antagonized by the Virus-Encoded NS1. *Journal of Virology*, 91(2): p. e01909-16.

46. Uehata T. and Akira S. 2013. *mRNA degradation by the endoribonuclease Regnase-1/ZC3H12a/MCPIP-1. Biochimica et Biophysica Acta*, 1829 (6-7): p. 708-13.

47. Vilas CK, Emery LE, Denchi EL, Miller KM. 2018. Caught with One's Zinc Fingers in the Genome Integrity Cookie Jar. *Trend in Genetics*. 34(4):313-325. doi: 10.1016/j.tig.2017.12.011. Epub 2018 Jan 19. PMID: 29370947; PMCID: PMC5878116.

48. Villa N, Do A, Hershey JW, Fraser CS. 2013. Human eukaryotic initiation factor 4G (eIF4G) protein binds to eIF3c, -d, and -e to promote mRNA recruitment to the ribosome. *Journal of Biological Chemistry*. 15;288(46):32932-40. doi: 10.1074/jbc.M113.517011. Epub 2013 Oct 3. PMID: 24092755; PMCID: PMC3829144.

49. Wang G. and Zheng C. 2021. Zinc finger proteins in the host-virus interplay: multifaceted functions based on their nucleic acid-binding property. *FEMS Microbiology Reviews*. 45(3).

50. Wang KT, Wang HH, Wu YY, Su YL, Chiang PY, Lin NY, Wang SC, Chang GD, Chang CJ. 2015. Functional regulation of Zfp36l1 and Zfp36l2 in response to lipopolysaccharide in mouse RAW264.7 macrophages. *Journal of Inflammation*.16;12:42. doi: 10.1186/s12950-015-0088-x. PMID: 26180518; PMCID: PMC4502546.

51. Wawro M, Kochan J, and Kasza A, The perplexities of the ZC3H12A self-mRNA regulation. *Acta Biochimica Polonica*, 63(3): p. 411-5.

52. Wu HY, Ke TY, Liao WY, Chang NY. 2013. Regulation of coronaviral poly(A) tail length during infection. *PLoS One*. 29;8(7):e70548. doi: 10.1371/journal.pone.0070548. PMID: 23923003; PMCID: PMC3726627.

53. Zhang B, Goraya MU, Chen N, Xu L, Hong Y, Zhu M and Chen JL .2020. Zinc Finger CCCH-Type Antiviral Protein 1 Restricts the Viral Replication by Positively Regulating Type I Interferon Response. *Frontiers in microbiology*. 11: 1912-1912.

54. Zhao Y, Song Z, Bai J, Liu X, Nauwynck H and Jiang P. 2019. ZAP, a CCCH-Type Zinc Finger Protein, Inhibits Porcine Reproductive and Respiratory Syndrome Virus Replication and Interacts with Viral Nsp9. *Journal of Virology*. 93(10).

55. Zhu M, Ma X, Cui X, Zhou J, Li C, Huang L, Shang Y, Cheng Z. 2017.Inhibition of avian tumor virus replication by CCCH-type zinc finger antiviral protein. *Oncotarget*. 19;8(35):58865-58871. doi: 10.18632/oncotarget.19378. PMID: 28938603; PMCID: PMC5601699.

56. Zhu M., Zhou J, Liang Y, Nair V, Yao Y and Cheng Z. 2020. CCCH-type zinc finger antiviral protein mediates antiviral immune response by activating T cells. *Journal of Leukocyte Biology*. 107(2): 299-307.

57. Zhu Y, Chen G, Lv F, Wang X, Ji X, Xu Y, Sun J, Wu L, Zheng YT, Gao G. 2011. Zinc-finger antiviral protein inhibits HIV-1 infection by selectively targeting multiply spliced viral mRNAs for degradation. *Proceedings of the National Academy of Sciences of the United States of America*. 20;108(38):15834-9. doi: 10.1073/pnas.1101676108. Epub 2011 Aug 29. PMID: 21876179; PMCID: PMC3179061.

489   58.   Zhu Y, Wang X, Goff SP, Gao G. 2012. Translational repression precedes and is
490   required for ZAP-mediated mRNA decay. *The EMBO Journal*. 5;31(21):4236-46. doi:
491   10.1038/emboj.2012.271. Epub 2012 Sep 28. PMID: 23023399; PMCID:
492   PMC3492732.
493
494
495
496

Figure 1

Overexpression and knockdown of ZFP36L1 in HCT-8 cells

Wild type HCT8 wells (A), ZFP36L1 overexpressed HCT-8 cells with GFP marker (B), and ZFP36L1 knockdown HCT-8 cells with mCherry marker (C). Overexpression and knockdown of ZFP36L1 were performed by lentivirus transduction.
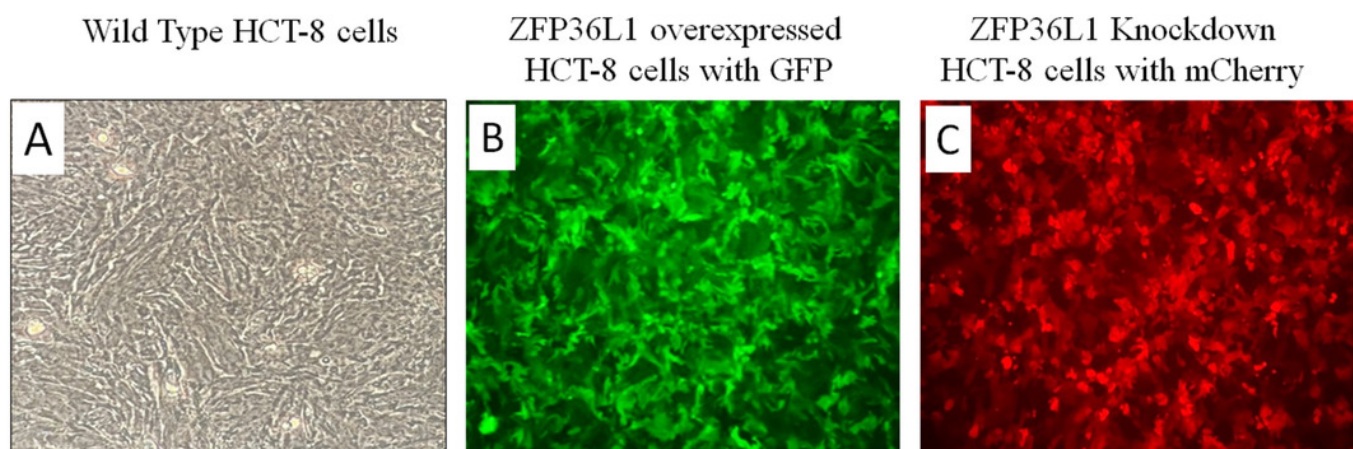
Figure 2

Western blot for confirming ZFP36L1 overexpression and knockdown in HCT-8 cells

Cell lysate for wild type HCT-8 cell (A), ZFP36L1 overexpressed (B) and ZFP36L1 knockdown (C) were separated with 12% resolving SDS PAGE gel and transferred to PVDF membrane. Proteins on the membrane were detected with an anti-ZFP36L1 antibody and anti- βactin antibody with HRP-conjugated secondary antibodies.
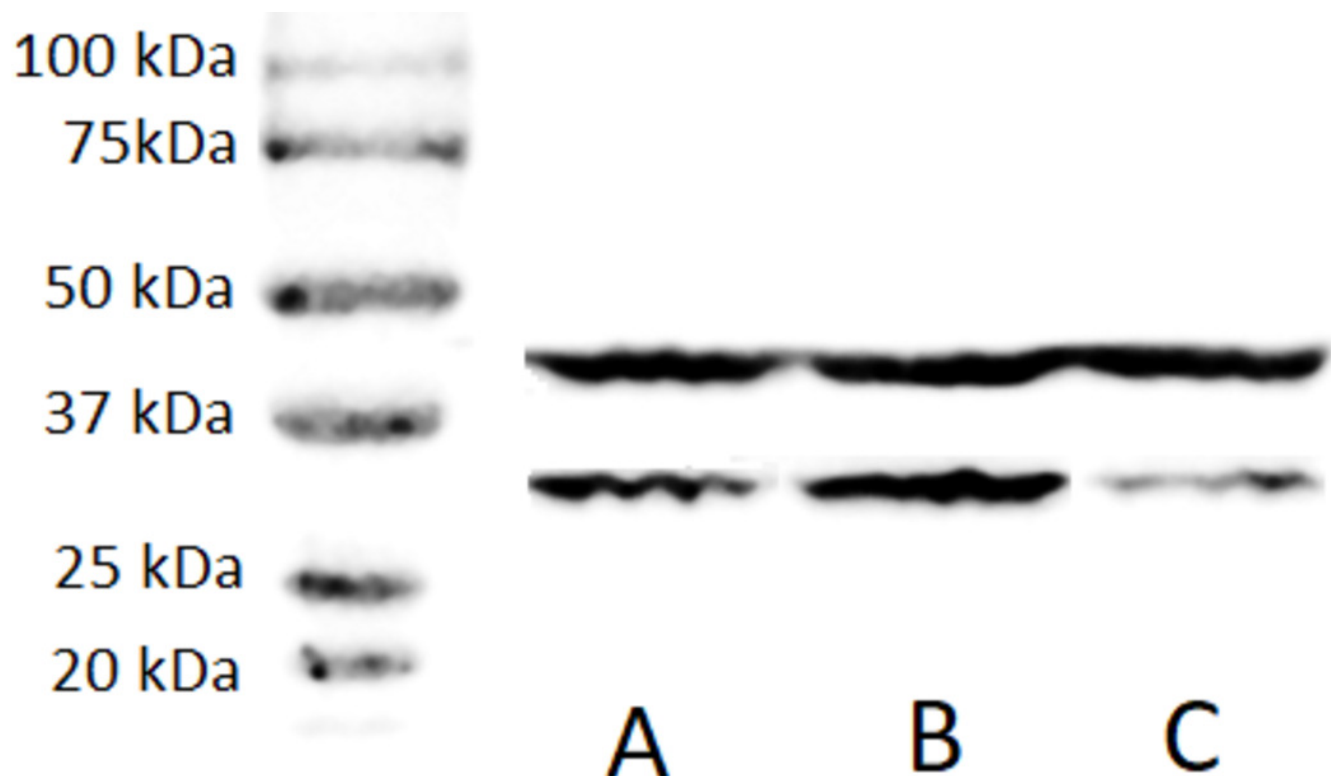
Figure 3

Relative quantification of ZFP36L1 expression in HCT-8 cell following its overexpression and knockdown

Cell lysate for wild-type HCT-8 cell, ZFP36L1 overexpressed and ZFP36L1 knockdown was analyzed for ZFP36L1 and β actin using western blot. Band intensity for ZFP36L1 proteins was normalized with β actin using ImageJ software. A significant difference in ZFP36L1 expression in ZFP36L1 overexpressed and knockdown cells compared to wild-type cells was estimated using a paired T-test. Asterisks are showing significant differences in ZFP36L1 expression.
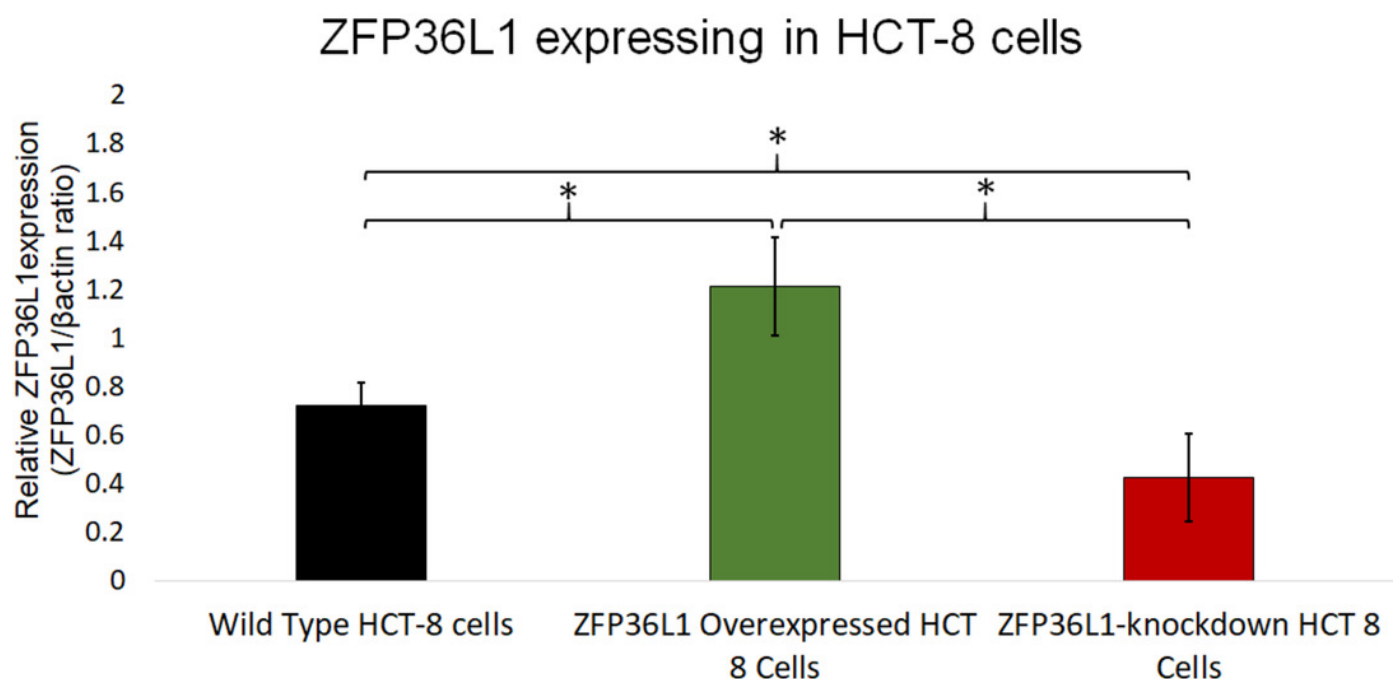
Figure 4

Effect of ZFP36L1 on HCT-8 cells viability

The effect of ZFP36L1 overexpression and its knockdown on cell viability was measured by trypan blue exclusion assay. Wild type, ZFP36L1 overexpressed and ZFP36L1 knockdown cells were individually seeded in 6 well plates. After 96 hours post-seeding, cells were detached and stained with 0.4% trypan blue to determine the percent viability. Changes in cell viability following ZFP36L1 overexpression or its knockdown compared to wild-type cells was estimated by paired T-test.
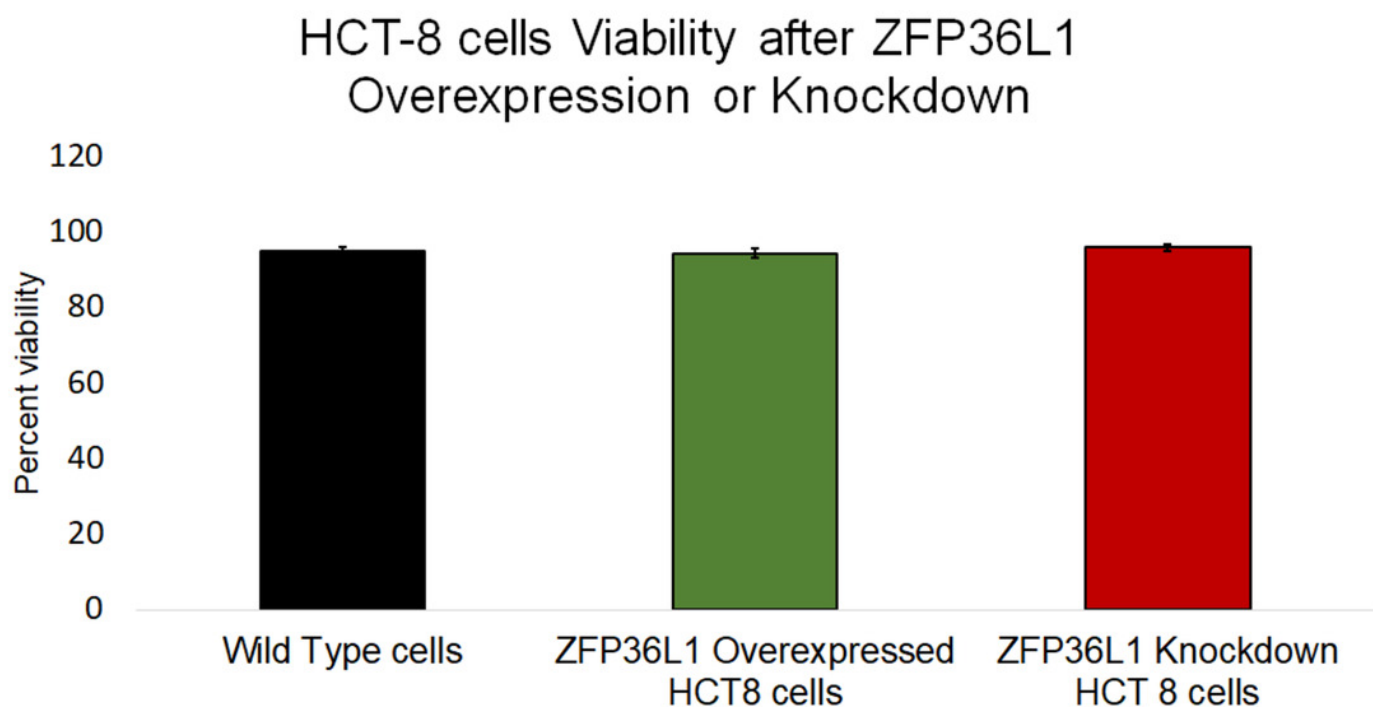
Figure 5

Human coronavirus-OC43 titer in HCT-8 cells.

Wild type, ZFP36L1 overexpressed and ZFP36L1 knockdown HCT-8 cells were infected individually with HCoV-OC43 with 0.1 MOI. Supernatant from these cells was collected at 24 hours, 48 hours, 72 hours, and 96 hours p.i. and analyzed for virus titer. Asterisks are showing significant differences in virus titer.
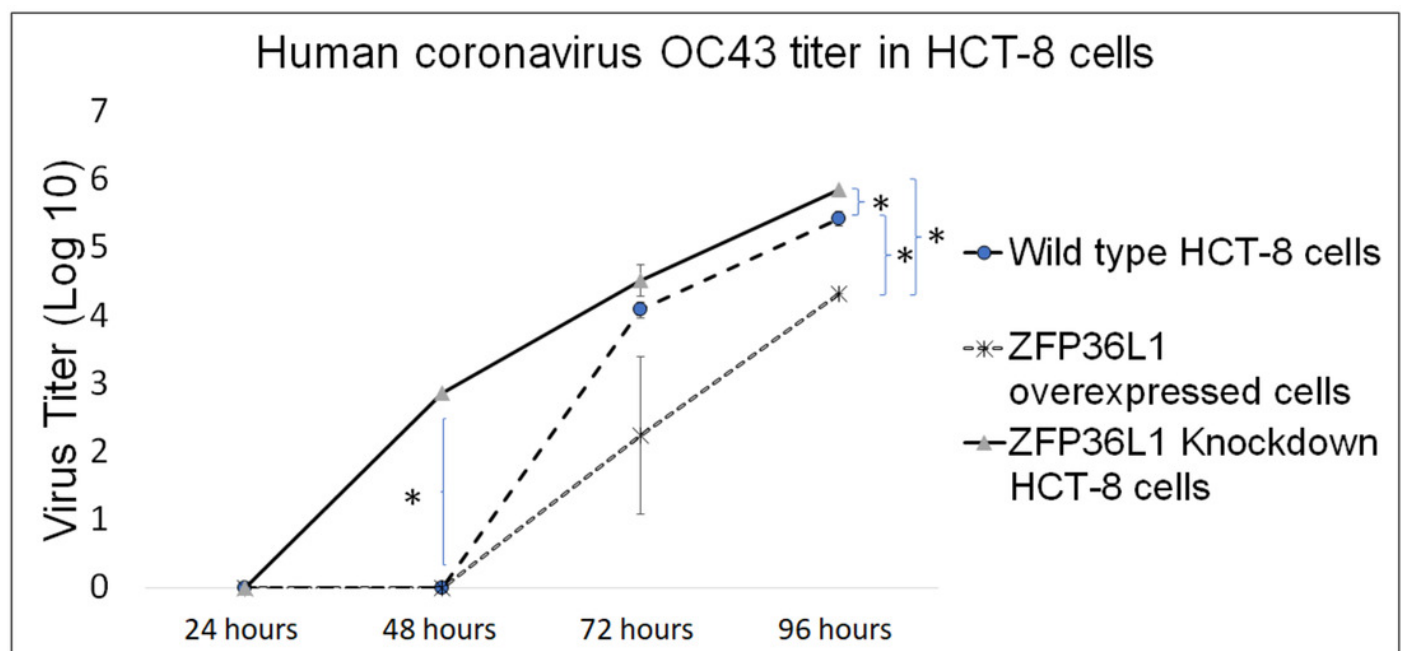
Figure 6

Effect of ZFP36L1 expression on Human coronavirus-OC43 induced cytopathic effect in HCT-8 cells

Wild type, ZFP36L1 overexpressed and ZFP36L1 knockdown HCT-8 cells were infected individually with HCoV-OC43 with 0.1 MOI. Cytopathic effect was observed at 72 hours p.i. at 40X magnification

Mock infected
Wild Type HCT-8 cells

HCoV-OC43 infected
Wild Type HCT-8 cells

HCoV-OC43 infected
ZFP36L1 overexpressed
HCT-8 cells

HCoV-OC43 infected
ZFP36L1 Knockdown
HCT-8 cells
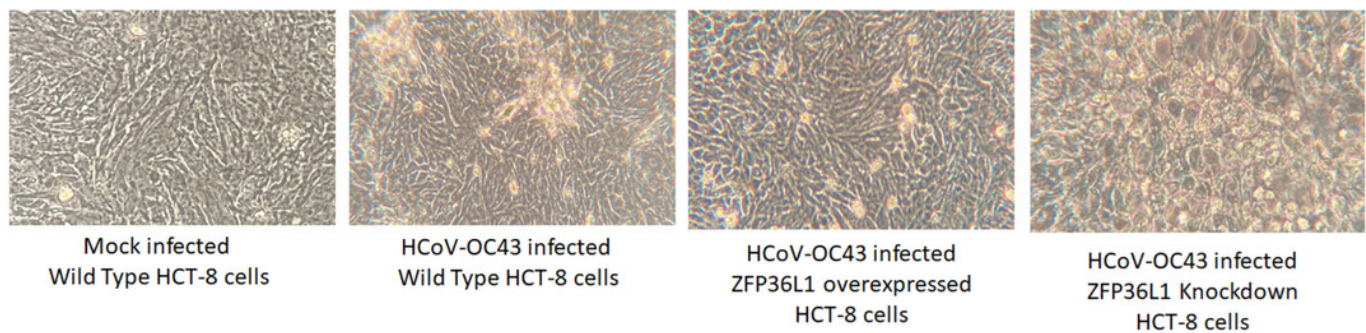
Figure 7

Effect of ZFP36L1 expression on Human coronavirus-OC43 replication

Wild-type, ZFP36L1 overexpressed and ZFP36L1 knockdown HCT-8 cells were infected individually with HCoV-OC43 with 0.1 MOI. Viral RNA was isolated from infected cells at 72 and 96 hours p.i. Isolated RNA was quantified using qPCR (for viral nucleocapsid). Fold change in nucleocapsid RNA in ZFP36L1 overexpressed and knockdown cells as compared to wild-type HCT-8 cells were estimated using paired T-test. Asterisks are showing significant differences in viral RNA.